ACS OMEGA

Article

Cite This: ACS Omega 2019, 4, 20486−20492

http://pubs.acs.org/journal/acsodf

Cauliflower-like Nickel with Polar $Ni(OH)_2/NiO_xF_y$ Shell To Decorate Copper Meshes for Efficient Oil/Water Separation

Zhi-Yong Luo,[†,‡,§] Shu-Shen Lyu,[†,§] and Dong-Chuan Mo*[,†,§]

[†]School of Materials, Sun Yat-sen University, Guangzhou 510275, P. R. China

[‡]School of Materials Science and Engineering, Nanyang Technological University, 50 Nanyang Avenue, Singapore 639798, Singapore

[§]Guangdong Engineering Technology Research Centre for Advanced Thermal Control Material and System Integration (ATCMSI), Guangzhou 510275, China

Supporting Information

ABSTRACT: In recent years, superhydrophilic and underwater superoleophobic membranes have shown promising results in advanced oil/water separation. However, these membranes still have some drawbacks, like tedious preparation process and instability, which hinder their application in oil/water separation. Accordingly, the development of a facile approach to prepare superhydrophilic membranes with excellent oil/water separation performance is still coveted. Here, a copper mesh decorated with cauliflower-like nickel (Cu mesh@CF-Ni) is synthesized via a facile one-step electrodeposition method. Due to the surface polar −OH and −O−Ni−F groups of the $Ni(OH)_2/NiO_xF_y$ shell of the cauliflower-like nickel (CF-Ni), this Cu mesh@CF-Ni displays superhydrophilic and underwater superoleophobic wettability. The results show that the Cu mesh@CF-Ni has excellent oil/water separation efficiency (higher than 99.2%) and ultrahigh water flux (around 20 L h^{-1} cm^{-2}). Moreover, it also displays good stability in a 10 wt % NaCl solution and 1 M NaOH solution for oil/water separation. By introducing the CF-Ni with polar $Ni(OH)_2/NiO_xF_y$ components onto the surface of the materials via a simple electrodeposition method, the materials will acquire the capability to not only achieve oil/water separation but also realize many other applications, like self-cleaning, underwater bubble manipulation, and fog harvesting.

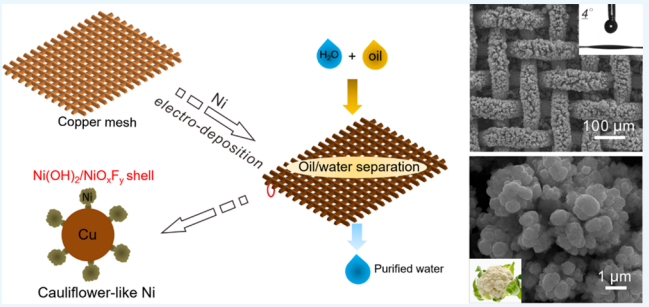

1. INTRODUCTION

Clean water is one of the most vital resources for social development. Unfortunately, clean water scarcity has been continuously worsening in recent decades due to increasing water pollution. Among the major concerns are various water contaminants, such as oil pollutants, which are mainly released into the environment by crude oil spill mishap[1,2] as well as industrial oily wastewater[3] from the oil refinery industry, cosmetics industry, and food processing industry. Traditional oil/water separation methods, such as air flotation,[4,5] centrifugation, chemical de-emulsification, absorption,[6−9] and polymeric membrane separation,[10,11] usually have drawbacks, such as high cost, low efficiency, and membrane fouling. Therefore, it is critical to develop advanced technologies or materials to address the ongoing oily wastewater crisis worldwide.

As widely known, materials with superwettability (i.e., superhydrophilicity or superhydrophobicity) have shown promising results for oil/water separation in the past decade.[12−16] Compared to superhydrophobic materials, superhydrophilic materials[17,18] have many advantages, like anticlogging, antifouling, and high efficiency, for the separation of oil/water mixtures. Decorating metal meshes with superhydrophilic species is the most popular method to design superhydrophilic membranes for advanced oil/water separation. To date, various metal meshes coated with superhydrophilic hydrogel,[19] copper,[20] $Cu(OH)_2$,[3] zeolite,[21] TiO_2,[13,22,23] Co_3O_4,[24] graphene oxide,[25] waste potato,[26] and nickel[27] have been reported, and they have exhibited good performance in oil/water separation. However, such materials still have drawbacks that hinder their industrial applications in oil/water separation, such as their tedious preparation process, expensive reagents, and thermal instability. Therefore, the development of a facile approach to prepare superhydrophilic membranes with superior oil/water separation ability is in great demand.

In our previous work, we synthesized superhydrophilic materials using a universal fluorine-induced superhydrophilicity (FIS) method through a simple and low-cost oxyfluorination process,[28] and those fluorine-induced superhydrophilic materials display excellent stability. By combining

Received: July 12, 2019
Accepted: October 22, 2019
Published: November 25, 2019

DOI: 10.1021/acsomega.9b02152
ACS Omega 2019, 4, 20486−20492

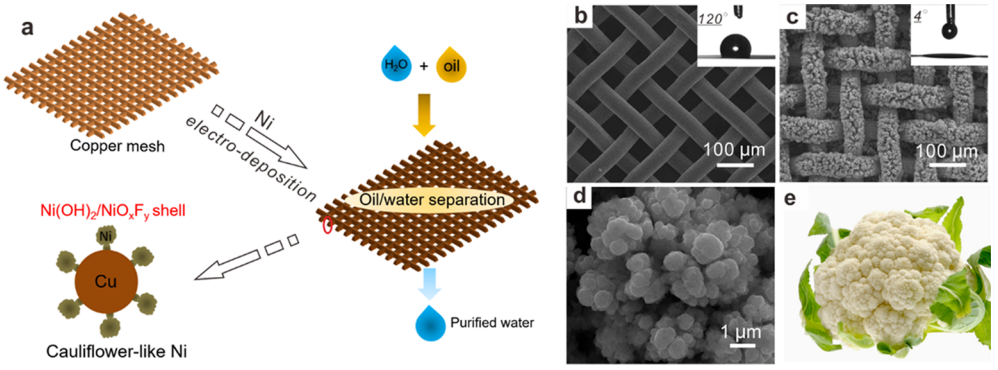

Figure 1. (a) Schematic of the preparation of the superhydrophilic copper mesh decorated with cauliflower-like nickel (Cu mesh@CF-Ni) and its application in oil/water separation. The scanning electron microscopy (SEM) characterization of (b) original copper mesh and (c) copper mesh after nickel electrodeposition. The inset images show the corresponding water contact angles. (d) Higher magnification SEM image of CF-Ni. (e) The image of a cauliflower.

the FIS and porous materials,[29,30] a facile approach to address the oily wastewater crisis can be implemented.

Here, Cu mesh@CF-Ni was synthesized via a simple one-step electrodeposition method in a fluorine-containing electrolyte. Different from our previous work,[27] we utilized nickel foam to replace nickel foil as the nickel resource to synthesized the Cu mesh@CF-Ni. Due to the large specific surface area of nickel foam, the speed of electrodeposition was enhanced, and the cauliflower-like nickel with fluorine-containing shell was obtained. The Cu mesh@CF-Ni was analyzed by scanning electron microscopy (SEM), transmission electron microscopy (TEM), X-ray diffraction (XRD), and X-ray photoelectron spectroscopy (XPS). Due to the surface polar −OH and −O− Ni−F groups of the $Ni(OH)_2/NiO_xF_y$ shell of CF-Ni, this Cu mesh@CF-Ni membrane displays superhydrophilic and underwater superoleophobic wettability. Then the Cu mesh@CF-Ni was evaluated in oil/water separation where it showed a high oil/water separation efficiency (above 99.2%) and ultrahigh water flux (around 20 L h^{-1} cm^{-2}). Also, the remarkable anticorrosive property of Cu mesh@CF-Ni in 10 wt % NaCl solution and 1 M NaOH solution in oil/water separation was confirmed using an electrochemical method.

2. RESULTS AND DISCUSSION

2.1. Characterization of Materials. The schematic illustration of the preparation of the superhydrophilic Cu mesh@CF-Ni via electrodeposition depicted in Figure 1a shows its application in oil/water separation. The SEM image shown in Figure 1b reveals that the surface of the original copper mesh is smooth and exhibits hydrophobicity (WCA = 120°). The Cu mesh@CF-Ni membrane was synthesized by using nickel foam as the nickel source during the nickel electrodeposition process (Figure S1). The electrodeposition process was drastic due to the large specific surface area of nickel foam, causing the irregular morphology of CF-Ni (Figure 1c,d). The Cu mesh@CF-Ni membrane displays superhydrophilic wettability (WCA = 4°, inset of Figure 1c), and the water droplet spreads out very fast on the Cu mesh@CF-Ni (see Figure S2). At the same time, the pore size of the Cu mesh@CF-Ni membrane was reduced after electrodeposition. The superhydrophilic wettability and the reduced pore size of the Cu mesh@CF-Ni membrane are beneficial to the subsequent oil/water separation. Noteworthy, the CF-Ni shows a cauliflower-like appearance (Figure 1d,e), which is similar to the structure reported in previous work.[31] This cauliflower-like structure with large roughness will benefit the formation of superhydrophilic materials.

To characterize the crystal structure and surface components of the Cu mesh@CF-Ni material, XRD and XPS analyses were conducted. The XRD spectrum of the Cu mesh@CF-Ni material shown in Figure 2a reveals that it is composed of Cu

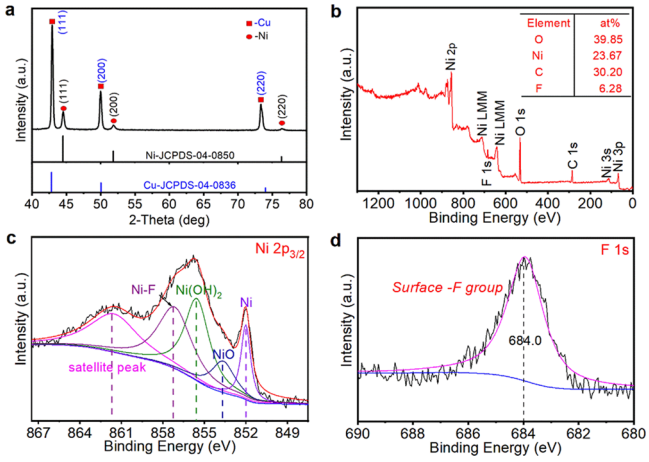

Figure 2. Analysis of the components of the Cu mesh@CF-Ni material. (a) X-ray diffraction (XRD) analysis of Cu mesh@CF-Ni. (b) Full X-ray photoelectron spectroscopy (XPS) spectrum and higher resolution (c) Ni $2p_{3/2}$ and (d) F 1s spectra of Cu mesh@CF-Ni.

and Ni, which is consistent with the standard cards (JCPDS-04-0836 and JCPDS-04-0850, respectively). Thus, the major component of CF-Ni is the metal Ni. As shown in Figure 2b, the surface of CF-Ni consists of four kinds of elements, namely, 39.85% O, 23.67% Ni, 30.20% C, and 6.28% F. The surface F and O come from the surface oxidation and fluoridation in the nickel electrodeposition. Additionally, as shown in Figure 2c, after the peak splitting of Ni $2p_{3/2}$, the surface Ni species are composed of metal Ni, NiO, $Ni(OH)_2$, and NiF_n, which have been confirmed at 852.0,[32] 853.7,[33] 855.5,[34] and 857.6 eV,[35] respectively. Also, the binding energy of F 1s in Figure 2d was determined to be about 684.0 eV, fitting the typical value of surface F species.[36] Therefore, the CF-Ni is composed of a $Ni(OH)_2/NiO/NiF_n$ shell and a Ni metal core.

DOI: 10.1021/acsomega.9b02152
ACS Omega 2019, 4, 20486−20492

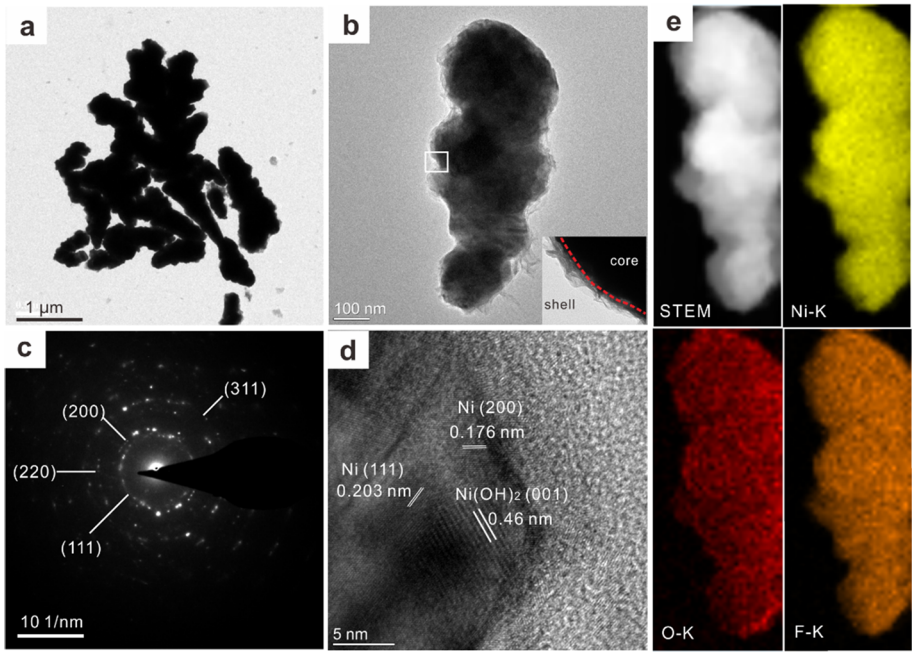

Figure 3. Characterization of the CF-Ni unit by transmission electron microscopy (TEM). (a,b) TEM images of CF-Ni units; the inset image of panel (b) shows the core−shell structure. (c) SAED and (d) HR-TEM analysis of the CF-Ni unit. (e) STEM characterization and corresponding element mapping of three kinds of elements, namely, Ni, O, and F.

We further examined the CF-Ni unit by TEM analysis. The TEM image shown in Figure 3a reveals the irregular appearance of the CF-Ni unit, which consists of a rough shell (Figure 3b). This structure can greatly increase the specific surface area, forming a thicker layer of adsorbed water for advanced oil/water separation. Additionally, the selected area electron diffraction (SAED) pattern of the CF-Ni unit indicated that the major ingredient of CF-Ni is metal Ni (Figure 3c), which is consistent with the result of the XRD analysis. The high resolution TEM (HR-TEM) image of the CF-Ni unit, shown in Figure 3d, reveals lattice parameters of 0.203, 0.176, and 0.46 nm, which are attributed to Ni (111),[37] Ni (200) (JCPDS-04-0850), and $Ni(OH)_2$ (001),[38] respectively. According to a previous report, NiO and NiF_n can combine with each other to form amorphous NiO_xF_y.[35] Thus, the lattice parameters of NiO and NiF_n do not correspond to those in Figure 3d. Given the interaction between NiO and NiF_n, the functional $Ni(OH)_2/NiO/NiF_n$ shell can be expressed as $Ni(OH)_2/NiO_xF_y$ with polar terminal groups in the form of −O−Ni−F (Figure 2c,d) and −OH (Figure S3). Additionally, the image in Figure 3e shows that Ni, O, and F are evenly distributed. Due to the surface polar −OH and −O−Ni−F groups of the $Ni(OH)_2/NiO_xF_y$ shell of CF-Ni, this Cu mesh@CF-Ni exhibits superhydrophilicity.

2.2. Wettability of Cu mesh@CF-Ni. It is widely known that the wettability of the membrane has a crucial role in oil/water separation applications.[39,40] As mentioned above, the Cu mesh@CF-Ni exhibits superhydrophilicity. It is beneficial to form an adsorbed water layer to enhance the oil/water separation efficiency. However, this efficiency also relies on its underwater oleophobicity. In this section, we analyzed the underwater oleophobicity of the Cu mesh@CF-Ni as depicted in Figure 4a, using a manmade glass tank (Figure 4b). The underwater adhesive effect between the oil droplet and the Cu mesh@CF-Ni membrane is illustrated in Figure 4c. The shape of the oil droplet remained almost the same when it left the

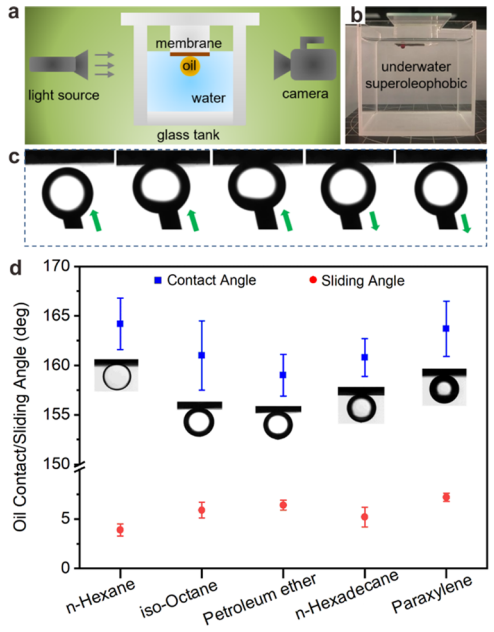

Figure 4. (a) Schematic illustration of the analysis of the underwater oil contact angle (OCA) and oil sliding angle (OSA). (b) The corresponding real device. (c) Underwater oil adhesive effect of the Cu mesh@CF-Ni membrane. (d) The OCAs and OSAs of five selected oils on the Cu mesh@CF-Ni membrane.

surface of Cu mesh@CF-Ni, indicating that the adhesive force between the oil droplet and the Cu mesh@CF-Ni is negligible. Also, the OCAs and OSAs of five selected oils on the Cu mesh@CF-Ni membrane were measured (Figure 4d). It is established that the OCA is above 155° and the OSA is below 10° for each oil. According to previous reports,[21,23,41] this superhydrophilic Cu mesh@CF-Ni material displays underwater superoleophobicity with low oil adhesion.

DOI: 10.1021/acsomega.9b02152
ACS Omega 2019, 4, 20486−20492

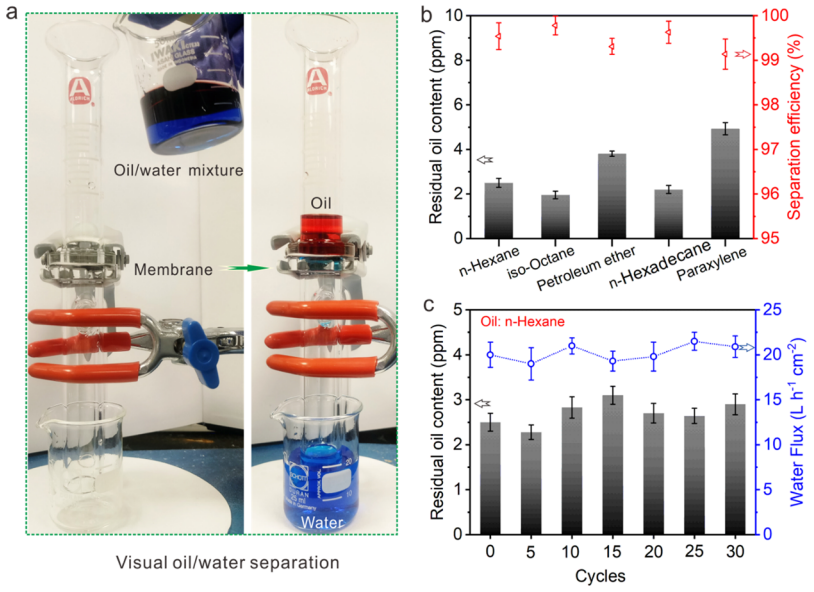

Figure 5. Oil/water separation experiments with the Cu mesh@CF-Ni. (a) The visual oil/water separation experiment. The water and oil were dyed with methylene blue and oil red, respectively. (b) The residual oil content in the separated water and the corresponding separation efficiency for the five selected oils. (c) The recycle experiments and the corresponding water flux of the Cu mesh@CF-Ni membrane.

2.3. Oil/Water Separation. During the oil/water separation process, a series of oil/water mixtures were separated once with this Cu mesh@CF-Ni membrane, and then the residual oil concentration in the separated water was measured. The separation efficiency was calculated as previously described[19]

$$R(\%) = (1 - C_p/C_0) \times 100 \quad (1)$$

Figure 5a illustrates the visual oil/water separation process. To illustrate it more clearly, the oil and water are dyed red and blue, respectively. Water permeated through the membrane immediately, and oil was retained above (see Movie S1). The residual oil contents of the five selected oils were below 5 ppm, and the separation efficiency was above 99.2%. The Cu mesh@CF-Ni membrane showed excellent oil/water separation performance (Figure 5b). Then its durability was evaluated by performing 30 cycles of hexane/water separation, which revealed that the Cu mesh@CF-Ni has good durability. The water flux was around 20 L h^{-1} cm^{-2}, which is much higher than that previously reported.[3,42−44]

2.4. Anticorrosive Experiments. Due to the corrosivity of industrial wastewater, the corrosive solution might destroy the micro/nanostructures as well as the wettability of membranes. Therefore, the anticorrosion properties of membranes are important to the industrial oil/water separation. Here, an electrochemical method was used to assess the stability of the Cu mesh@CF-Ni membrane for oil/water separation in 1 M NaOH, 10 wt % NaCl solutions, and 1 M HCl. The Tafel polarization curves of the Cu mesh@CF-Ni membrane in four kinds of solutions are shown in Figure 6a, and the corresponding corrosion current density are summarized in Table S1. The corrosion current density of the Cu mesh@CF-Ni membrane in 1 M HCl solution is 501.2 μA cm^{-2}, which is significantly larger than those in H_2O (1.6 μA cm^{-2}), 1 M NaOH (25.1 μA cm^{-2}), and 10 wt % NaCl (31.6 μA cm^{-2}), indicating that the Cu mesh@CF-Ni membrane has poor stability in the 1 M HCl solution. After being immersed in the three aforementioned solutions for 1 h, the micro/nanostructures of CF-Ni were destroyed in 1 M HCl solution but remained the same in 10 wt % NaCl solutions and 1 M NaOH solutions (Figure S4). Thereafter, oil/water separation experiments were conducted in 10 wt % NaCl solution and 1 M NaOH solution. In Figure 6b, the Cu mesh@CF-Ni membrane also showed underwater superoleophobicity in 1 M NaOH and 10 wt % NaCl solutions, and the separation efficiencies were above 98.5 and 99%, respectively. Additionally, the Cu mesh@CF-Ni membrane has

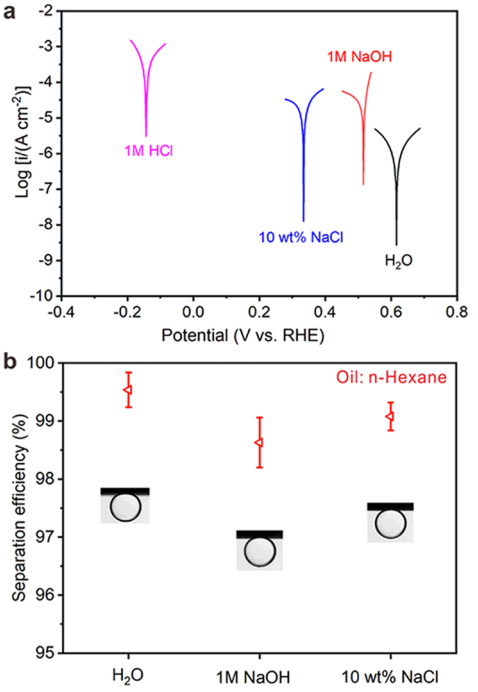

Figure 6. Anticorrosion experiments with the Cu mesh@CF-Ni membrane. (a) Electrochemical corrosion measurements of the Cu mesh@CF-Ni membrane in solutions. (b) The oil/water separation efficiencies and the corresponding OCAs of the Cu mesh@CF-Ni membrane in water, 10 wt % NaCl solutions, and 1 M NaOH solution.

DOI: 10.1021/acsomega.9b02152
ACS Omega 2019, 4, 20486−20492

good stability in 10 wt % NaCl solution and 1 M NaOH solutions for oil/water separation.

3. CONCLUSIONS

In summary, we fabricated the Cu mesh@CF-Ni material via a facile electrodeposition method for application in advanced oil/water separation. This Cu mesh@CF-Ni membrane displays superhydrophilicity and underwater superoleophobic wettability due to the surface polar −OH and −O−Ni−F groups of the $Ni(OH)_2/NiO_xF_y$ shell of the CF-Ni unit. The experimental results demonstrated that the Cu mesh@CF-Ni membrane has high oil/water separation efficiency (>99.2%) with strong durability and ultrahigh water flux (around 20 L h^{-1} cm^{-2}). Additionally, it displays good stability in 10 wt % NaCl solution and 1 M NaOH solution. By introducing the CF-Ni with polar $Ni(OH)_2/NiO_xF_y$ components onto the surface of the materials by a simple electrodeposition method, these materials acquire the capability for many other applications, such as self-cleaning,[45] underwater bubble manipulation,[46] and fog harvesting.[47,48]

4. EXPERIMENTAL DETAILS

4.1. Preparation of Cu mesh@CF-Ni. The 400# copper mesh (purity ≥99.5%) was cut into 3 cm × 3 cm pieces and cleaned by an ultrasonic cleaner (40 kHz) with 10 wt % H_2SO_4, deionized water, ethanol, and deionized water.[49] The Cu mesh@CF-Ni was obtained using an electrochemical cell with a two-electrode distance of 1.5 cm. The cathode and the anode were the cleaned copper mesh and a piece of nickel foam (3 cm × 3 cm size, 99.7% purity), respectively. The electrolyte consisted of 99.85 wt % H_2O and 0.15 wt % NH_4F. The electrodeposition was carried out at 4 V for 1 h, and the electrolyte was kept at a temperature of 25 °C.

4.2. Materials Characterization. Characterization of the morphology of the Cu mesh@CF-Ni material was carried out by SEM, using a JSM-6510LV scanning electron microscope (JEOL Ltd., Tokyo, Japan), and TEM, using a Tecnai G2 F30 transmission electron microscope (FEI Co., Hillsboro, OR, USA). The surface components were analyzed by XPS using an ESCALAB250 X-ray photoelectron spectrometer (Thermo Fisher Scientific, Waltham, MA, USA). The crystal structure was confirmed by XRD analysis using an Empyrean X-ray diffractometer (Malvern Panalytical Inc., Malvern, U.K.). The water contact angle (WCA), underwater oil contact angle (OCA), underwater oil sliding angle (OSA), and underwater oil adhesive effect were measured with an OCA20 contact angle tester (Data Physics Instruments GmbH, Filderstadt, Germany). The dynamic water spreading effect on the interfaces was tested by a 5 μL deionized droplet and was monitored with a Phantom V.211 high-speed camera (Vision Research, Wayne, NJ, USA) by capturing at 3000 fps.

4.3. Oil/Water Separation. Five oils (*n*-hexane, *n*-hexadecane, isooctane, paraxylene, and petroleum ether) were selected for the oil/water separation experiments. The oil/water mixture ratio is 10 (w_{water}/w_{oil} = 10). Two glass tubes (d = 1.5 cm) and a Cu mesh@CF-Ni placed between these tubes were fastened with a flange and clamps. When the mixture was filled into the tube, the water separated into a beaker below.

After separation, 1 M HCl was used to acidify the water in the lower tube (60 mL) to pH = 1−2, and 2 g of NaCl was added into the water to demulsify it. Then 40 mL of CCl_4 was used to extract twice, and anhydrous Na_2SO_4 was used to dry the extractant. Eventually, the oil concentration in CCl_4 was measured using an infrared oil concentration analyzer (OIL-8, China).[30,50]

4.4. Anticorrosive Experiments. The electrochemical corrosion measurements of Cu mesh@CF-Ni in corrosive solutions (i.e., 10 wt % NaCl, 1 M HCl, and1 M NaOH) were performed on a CHI760 workstation (CH Instruments Inc., Austin, TX, USA). The working, reference, and counter electrodes were the Cu mesh@CF-Ni, a saturated calomel electrode (SCE), and a Pt wire, respectively. Polarization curves were plotted by scanning the potential from (E −0.5 V) to (E +1.25 V) with a scan rate of 1 mV s^{-1}, where E is the open circuit potential. Then the oil/solution mixture ($w_{solution}/w_{oil}$ = 10, solution is 10 wt % NaCl or 1 M NaOH) was separated using the Cu mesh@CF-Ni; the results were compared to those of the oil/water mixture separation.

■ ASSOCIATED CONTENT

Supporting Information

The Supporting Information is available free of charge at https://pubs.acs.org/doi/10.1021/acsomega.9b02152.

Schematic illustration of the preparation process, water droplet test, O 1s spectra, data of electrochemical corrosion measurements, SEM images (PDF)

Movie of visual oil/water separation (MP4)

■ AUTHOR INFORMATION

Corresponding Author

*E-mail: modongch@mail.sysu.edu.cn. Tel: +86-20-84113985.

ORCID

Dong-Chuan Mo: 0000-0003-1188-1432

Notes

The authors declare no competing financial interest.

■ ACKNOWLEDGMENTS

This work was supported by the Natural Science Foundation of China (No. 51876226) and the Guangdong Natural Science Foundation (No.2014A030312009, No. 2018A030313482).

■ REFERENCES

(1) Kintisch, E. An audacious decision in crisis gets cautious praise. *Science* **2010**, *329*, 735−736.

(2) Worton, D. R.; Zhang, H.; Isaacman-VanWertz, G.; Chan, A. W. H.; Wilson, K. R.; Goldstein, A. H. Comprehensive chemical characterization of hydrocarbons in nist standard reference material 2779 gulf of mexico crude oil. *Environ. Sci. Technol.* **2015**, *49*, 13130−13138.

(3) Zhang, F.; Zhang, W. B.; Shi, Z.; Wang, D.; Jin, J.; Jiang, L. Nanowire-haired inorganic membranes with superhydrophilicity and underwater ultralow adhesive superoleophobicity for high-efficiency oil/water separation. *Adv. Mater.* **2013**, *25*, 4192−4198.

(4) Temesgen, T.; Bui, T. T.; Han, M.; Kim, T. I.; Park, H. Micro and nanobubble technologies as a new horizon for water-treatment techniques: A review. *Adv. Colloid Interface Sci.* **2017**, *246*, 40−51.

(5) Heeres, A. S.; Heijnen, J. J.; van der Wielen, L. A. M.; Cuellar, M. C. Gas bubble induced oil recovery from emulsions stabilised by yeast components. *Chem. Eng. Sci.* **2016**, *145*, 31−44.

(6) Ge, J.; Shi, L.-A.; Wang, Y.-C.; Zhao, H.-Y.; Yao, H.-B.; Zhu, Y.-B.; Zhang, Y.; Zhu, H.-W.; Wu, H.-A.; Yu, S.-H. Joule-heated graphene-wrapped sponge enables fast clean-up of viscous crude-oil spill. *Nat. Nanotechnol.* **2017**, *12*, 434−440.

DOI: 10.1021/acsomega.9b02152
ACS Omega 2019, 4, 20486−20492

(7) Si, Y.; Fu, Q.; Wang, X.; Zhu, J.; Yu, J.; Sun, G.; Ding, B. Superelastic and superhydrophobic nanofiber-assembled cellular aerogels for effective separation of oil/water emulsions. *ACS Nano* **2015**, *9*, 3791−3799.
(8) Gao, X.; Zhou, J.; Du, R.; Xie, Z.; Deng, S.; Liu, R.; Liu, Z.; Zhang, J. Robust superhydrophobic foam: A graphdiyne-based hierarchical architecture for oil/water separation. *Adv. Mater.* **2016**, *28*, 168−173.
(9) Si, Y.; Yu, J.; Tang, X.; Ge, J.; Ding, B. Ultralight nanofibre-assembled cellular aerogels with superelasticity and multifunctionality. *Nat. Commun.* **2014**, *5*, 5802.
(10) Ou, R.; Wei, J.; Jiang, L.; Simon, G. P.; Wang, H. Robust Thermoresponsive Polymer Composite Membrane with Switchable Superhydrophilicity and Superhydrophobicity for Efficient Oil-Water Separation. *Environ. Sci. Technol.* **2016**, *50*, 906−914.
(11) Tao, M.; Xue, L.; Liu, F.; Jiang, L. An intelligent superwetting PVDF membrane showing switchable transport performance for oil/water separation. *Adv. Mater.* **2014**, *26*, 2943−2948.
(12) Gao, X.; Xu, L.-P.; Xue, Z.; Feng, L.; Peng, J.; Wen, Y.; Wang, S.; Zhang, X. Dual-scaled porous nitrocellulose membranes with underwater superoleophobicity for highly efficient oil/water separation. *Adv. Mater.* **2014**, *26*, 1771−1775.
(13) Gao, C.; Sun, Z.; Li, K.; Chen, Y.; Cao, Y.; Zhang, S.; Feng, L. Integrated oil separation and water purification by a double-layer TiO_2-based mesh. *Energy Environ. Sci.* **2013**, *6*, 1147−1151.
(14) Yang, S.; Si, Y.; Fu, Q.; Hong, F.; Yu, J.; Al-Deyab, S. S.; El-Newehy, M.; Ding, B. Superwetting hierarchical porous silica nanofibrous membranes for oil/water microemulsion separation. *Nanoscale* **2014**, *6*, 12445−12449.
(15) Yanlong, S.; Wu, Y.; Xiaojuan, F.; Yongsheng, W.; Guoren, Y.; Shuping, J. Fabrication of superhydrophobic-superoleophilic copper mesh via thermal oxidation and its application in oil−water separation. *Appl. Surf. Sci.* **2016**, *367*, 493−499.
(16) Tenjimbayashi, M.; Sasaki, K.; Matsubayashi, T.; Abe, J.; Manabe, K.; Nishioka, S.; Shiratori, S. A biologically inspired attachable, self-standing nanofibrous membrane for versatile use in oil-water separation. *Nanoscale* **2016**, *8*, 10922−10927.
(17) Long, Y.; Shen, Y.; Tian, H.; Yang, Y.; Feng, H.; Li, J. Superwettable Coprinus comatus coated membranes used toward the controllable separation of emulsified oil/water mixtures. *J. Membr. Sci.* **2018**, *565*, 85−94.
(18) Wang, X.; Li, M.; Shen, Y.; Yang, Y.; Feng, H.; Li, J. Facile preparation of loess-coated membranes for multifunctional surfactant-stabilized oil-in-water emulsion separation. *Green Chem.* **2019**, *21*, 3190−3199.
(19) Xue, Z.; Wang, S.; Lin, L.; Chen, L.; Liu, M.; Feng, L.; Jiang, L. A novel superhydrophilic and underwater superoleophobic hydrogel-coated mesh for oil/water separation. *Adv. Mater.* **2011**, *23*, 4270−4273.
(20) Zhang, E.; Cheng, Z.; Lv, T.; Qian, Y.; Liu, Y. Anti-corrosive hierarchical structured copper mesh film with superhydrophilicity and underwater low adhesive superoleophobicity for highly efficient oil-water separation. *J. Mater. Chem. A* **2015**, *3*, 13411−13417.
(21) Wen, Q.; Di, J.; Jiang, L.; Yu, J.; Xu, R. Zeolite-coated mesh film for efficient oil-water separation. *Chem. Sci.* **2013**, *4*, 591−595.
(22) Lin, X.; Chen, Y.; Liu, N.; Cao, Y.; Xu, L.; Zhang, W.; Feng, L. In situ ultrafast separation and purification of oil/water emulsions by superwetting TiO_2 nanocluster-based mesh. *Nanoscale* **2016**, *8*, 8525−8529.
(23) Zhou, C.; Cheng, J.; Hou, K.; Zhao, A.; Pi, P.; Wen, X.; Xu, S. Superhydrophilic and underwater superoleophobic titania nanowires surface for oil repellency and oil/water separation. *Chem. Eng. J.* **2016**, *301*, 249−256.
(24) Chen, Y.; Wang, N.; Guo, F.; Hou, L.; Liu, J.; Liu, J.; Xu, Y.; Zhao, Y.; Jiang, L. A Co_3O_4 nano-needle mesh for highly efficient, high-flux emulsion separation. *J. Mater. Chem. A* **2016**, *4*, 12014−12019.
(25) Liu, Y.-Q.; Zhang, Y.-L.; Fu, X.-Y.; Sun, H.-B. Bioinspired underwater superoleophobic membrane based on a graphene oxide coated wire mesh for efficient oil/water separation. *ACS Appl. Mater. Interfaces* **2015**, *7*, 20930−20936.
(26) Li, J.; Li, D.; Yang, Y.; Li, J.; Zha, F.; Lei, Z. A prewetting induced underwater superoleophobic or underoil (super) hydrophobic waste potato residue-coated mesh for selective efficient oil/water separation. *Green Chem.* **2016**, *18*, 541−549.
(27) Luo, Z.-Y.; Chen, K.-X.; Wang, Y.-Q.; Wang, J.-H.; Mo, D.-C.; Lyu, S.-S. Superhydrophilic nickel nanoparticles with core−shell structure to decorate copper mesh for efficient oil/water separation. *J. Phys. Chem. C* **2016**, *120*, 12685−12692.
(28) Luo, Z.-Y.; Chen, K.-X.; Mo, D.-C.; Lyu, S.-S. A new route for surface modification: Fluorine-induced superhydrophilicity. *J. Phys. Chem. C* **2016**, *120*, 11882−11888.
(29) Jiang, B.; Chen, Z.; Dou, H.; Sun, Y.; Zhang, H.; Gong, Z. Q.; Zhang, L. Superhydrophilic and underwater superoleophobic Ti foam with fluorinated hierarchical flower-like TiO 2 nanostructures for effective oil-in-water emulsion separation. *Appl. Surf. Sci.* **2018**, *456*, 114−123.
(30) Luo, Z.-Y.; Lyu, S.-S.; Wang, Y.-Q.; Mo, D.-C. Fluorine-Induced Superhydrophilic Ti Foam with Surface Nanocavities for Effective Oil-in-Water Emulsion Separation. *Ind. Eng. Chem. Res.* **2017**, *56*, 699−707.
(31) Wang, J.; Wang, H. Integrated device based on cauliflower-like nickel hydroxide particles−coated fabrics with inverse wettability for highly efficient oil/hot alkaline water separation. *J. Colloid Interface Sci.* **2019**, *534*, 228−238.
(32) Yang, H.; Xu, H.; Li, M.; Zhang, L.; Huang, Y.; Hu, X. Assembly of $NiO/Ni(OH)_2$/PEDOT nanocomposites on contra wires for fiber-shaped flexible asymmetric supercapacitors. *ACS Appl. Mater. Interfaces* **2016**, *8*, 1774−1779.
(33) Lee, D. U.; Fu, J.; Park, M. G.; Liu, H.; Ghorbani Kashkooli, A.; Chen, Z. Self-Assembled $NiO/Ni(OH)_2$ Nanoflakes as Active Material for High-Power and High-Energy Hybrid Rechargeable Battery. *Nano Lett.* **2016**, *16*, 1794−1802.
(34) Zhang, C.; Qian, L.; Zhang, K.; Yuan, S.; Xiao, J.; Wang, S. Hierarchical porous Ni/NiO core-shells with superior conductivity for electrochemical pseudo-capacitors and glucose sensors. *J. Mater. Chem. A* **2015**, *3*, 10519−10525.
(35) Yang, Y.; Li, L.; Ruan, G.; Fei, H.; Xiang, C.; Fan, X.; Tour, J. M. Hydrothermally Formed Three-Dimensional Nanoporous $Ni(OH)_2$ Thin-Film Supercapacitors. *ACS Nano* **2014**, *8*, 9622−9628.
(36) Yang, H. G.; Sun, C. H.; Qiao, S. Z.; Zou, J.; Liu, G.; Smith, S. C.; Cheng, H. M.; Lu, G. Q. Anatase TiO_2 single crystals with a large percentage of reactive facets. *Nature* **2008**, *453*, 638−641.
(37) He, L.; Liao, Z.-M.; Wu, H.-C.; Tian, X.-X.; Xu, D.-S.; Cross, G. L. W.; Duesberg, G. S.; Shvets, I. V.; Yu, D.-P. Memory and threshold resistance switching in Ni/NiO core-shell nanowires. *Nano Lett.* **2011**, *11*, 4601−4606.
(38) Shahid, M.; Liu, J.; Shakir, I.; Warsi, M. F.; Nadeem, M.; Kwon, Y.-U. Facile approach to synthesize $Ni(OH)_2$ nanoflakes on MWCNTs for high performance electrochemical supercapacitors. *Electrochim. Acta* **2012**, *85*, 243−247.
(39) Chu, Z.; Feng, Y.; Seeger, S. Oil/water separation with selective superantiwetting/superwetting surface materials. *Angew. Chem., Int. Ed.* **2015**, *54*, 2328−2338.
(40) Wang, B.; Liang, W.; Guo, Z.; Liu, W. Biomimetic super-lyophobic and super-lyophilic materials applied for oil/water separation: a new strategy beyond nature. *Chem. Soc. Rev.* **2015**, *44*, 336−361.
(41) Zhou, C.; Cheng, J.; Hou, K.; Zhu, Z.; Zheng, Y. Preparation of $CuWO_4$@Cu_2O film on copper mesh by anodization for oil/water separation and aqueous pollutant degradation. *Chem. Eng. J.* **2017**, *307*, 803−811.
(42) Li, Q.; Deng, W.; Li, C.; Sun, Q.; Huang, F.; Zhao, Y.; Li, S. High-Flux Oil/Water Separation with Interfacial Capillary Effect in Switchable Superwetting $Cu(OH)_2$@ZIF-8 Nanowire Membranes. *ACS Appl. Mater. Interfaces* **2018**, *10*, 40265−40273.
(43) Li, J.; Xu, C.; Guo, C.; Tian, H.; Zha, F.; Guo, L. Underoil superhydrophilic desert sand layer for efficient gravity-directed water-

DOI: 10.1021/acsomega.9b02152
ACS Omega 2019, 4, 20486−20492

in-oil emulsions separation with high flux. *J. Mater. Chem. A* **2018**, *6*, 223−230.
(44) Zhang, J. Q.; Xue, Q. Z.; Pan, X. L.; Jin, Y. K.; Lu, W. B.; Ding, D. G.; Guo, Q. K. Graphene oxide/polyacrylonitrile fiber hierarchical-structured membrane for ultra-fast microfiltration of oil-water emulsion. *Chem. Eng. J.* **2017**, *307*, 643−649.
(45) Banerjee, S.; Dionysiou, D. D.; Pillai, S. C. Self-cleaning applications of TiO_2 by photo-induced hydrophilicity and photocatalysis. *Appl. Catal. B* **2015**, *176-177*, 396−428.
(46) Yu, C.; Cao, M.; Dong, Z.; Wang, J.; Li, K.; Jiang, L. Spontaneous and Directional Transportation of Gas Bubbles on Superhydrophobic Cones. *Adv. Funct. Mater.* **2016**, *26*, 3236−3243.
(47) Bai, H.; Wang, L.; Ju, J.; Sun, R.; Zheng, Y.; Jiang, L. Efficient water collection on integrative bioinspired surfaces with star-shaped wettability patterns. *Adv. Mater.* **2014**, *26*, 5025−5030.
(48) Park, K.-C.; Kim, P.; Grinthal, A.; He, N.; Fox, D.; Weaver, J. C.; Aizenberg, J. Condensation on slippery asymmetric bumps. *Nature* **2016**, *531*, 78−82.
(49) Chen, Y.; Wang, X. M.; Lu, S. S.; Zhang, X. Formation of titanium oxide nanogrooves island arrays by anodization. *Electrochem. Commun.* **2010**, *12*, 86−89.
(50) Luo, Z.-Y.; Chen, K.-X.; Wang, J.-H.; Mo, D.-C.; Lyu, S.-S. Hierarchical nanoparticle-induced superhydrophilic and under-water superoleophobic Cu foam with ultrahigh water permeability for effective oil/water separation. *J. Mater. Chem. A* **2016**, *4*, 10566−10574.

DOI: 10.1021/acsomega.9b02152
ACS Omega 2019, 4, 20486−20492